VNWA3E – A Low Cost Vector Network Analyzer not only for Education

Prof. Dr. Thomas Baier
University of Applied Sciences Ulm
Prittwitzstrasse 10
89075 Ulm
Germany

Ulm, 30.4.2015

Part B: Unconventional Applications for the VNWA3

Introduction:

While the first part of this article series focused on the functional principle of the VNWA3, this second part will demonstrate possibilities leading to rather unconventional applications, some of which being not normally associated with VNWA usage. The VNWA's abilities to sweep very rapidly, to measure at very low frequencies and to support unconventional impedance measurement bridges e.g. for measuring extremely low impedances are being discussed. Moreover, the VNWA software's computational power is being demonstrated. For discussion of rather conventional RF applications of the VNWA the reader may be referred to [1].

1. Measurement Speed vs. Noise Floor

The VNWA3 signal sources being direct digital synthesizers (DDS) are very agile and can thus be swept very rapidly. Limiting sweep speed factors are data transfer times to the DDS chips, data acquisition times of the VNWA and ringing of the device under test (DUT). Particularly, narrow band components like crystal filters tend to ring upon changing input frequencies. Therefore such devices have to be swept slowly or with small frequency increments. Both can be done with the VNWA3 with different side effects.

Figure 1 shows three measurements on the same monolithic crystal filter (MCF), which has been selected for its very high out of band rejection. While the number of frequency points has been increased from blue (400) over green (4000) to red (64000), the time per data point has been decreased from blue (100ms) over green (3.3ms) to red (0.16ms). On the one hand, this demonstrates the VNWA's ability to measure at high speed of more than 6000 data points per second (red trace). This also demonstrates that there is a tradeoff between measurement speed and dynamic range. Like for any receiver, the noise floor level depends on the receiver's bandwidth, which in this case is basically the inverse of the measurement time per data point. Thus, doubling the time per data point will ideally lower the noise floor by 3dB. As the time per data point is increased by a factor of about 20 from the red to the green trace, the noise floor should drop by a factor of $3\mathrm{dB}\cdot\log_2(20)=13\mathrm{dB}$ which is about what is being observed. From the green trace to the blue trace the noise floor should again drop by $3\mathrm{dB}\cdot\log_2(30)\approx 15\mathrm{dB}$ to well below -100dB (black dashed line). At such a low noise floor, features of the filter stop band become visible.

トランジスタ技術 2016 年 1 月号～4 月号

USB ネットワーク・アナライザ VNWA3E のすべて<2>～<5>（原文）

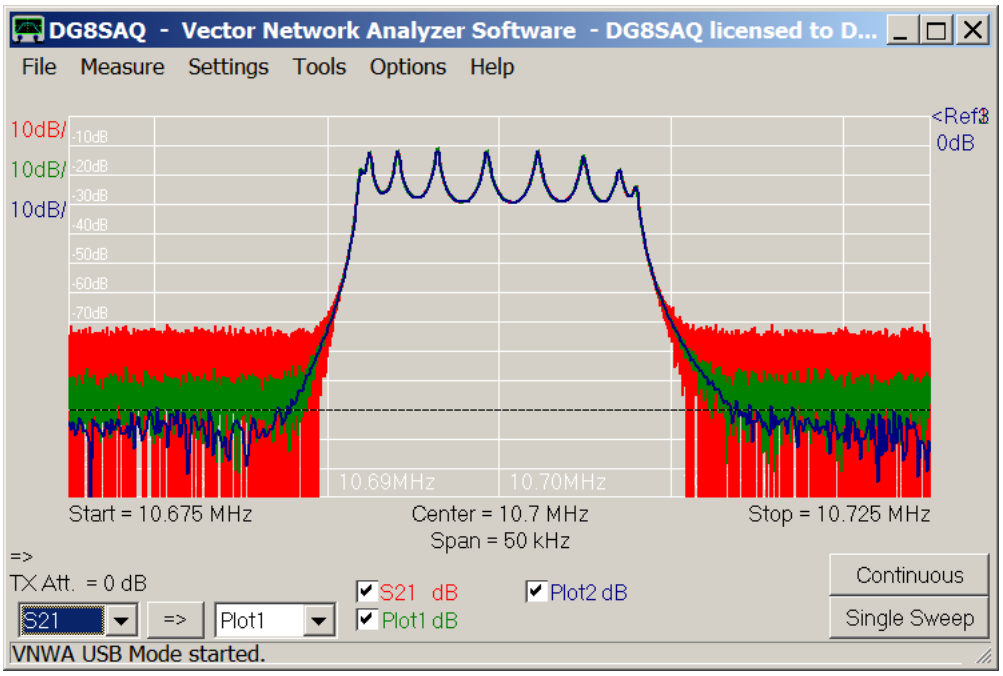

Figure 1: Monolithic crystal filter measured with three different settings. Red: 64000 points @ 0.16ms per point i.e. 10s measurement time; Green: 4000 points @ 3.3ms per point i.e. 13s measurement time; Blue: 400 points @ 100ms per point i.e. 40s measurement time. Clearly, the noise floor depends on the measurement time per point. The black dashed line indicates the -100dB level.

Fast sweeping is particularly interesting when tuning devices while observing the effect of tuning in real time. Using 500 frequency points per sweep, a sweep repetition rate of 5 sweeps per second is achieved including all overhead required from end of sweep to start of next sweep. This yields a comfortable resolution and a sweep speed sufficiently fast for real time tuning.

2. Very low frequency measurements

DDS frequency sources can be tuned to very low frequencies enabling the VNWA3 to perform measurements well into the audio frequency range. In the following, the VNWA's capability to measure at frequencies as low as 200Hz is demonstrated.

2.1 Parasitics and ESR of tantalum capacitor

Capacitors with large capacitance values have to be evaluated at low frequencies. Figure 2 shows the measurement setup with a 22uF wired tantalum capacitor connected to the TX port with its 2,5cm long lead wires soldered to a BNC connector. For the measurement, the VNWA TX port was SOL-calibrated with the also visible BNC SOL-calibration standards.

Figure 2: Measurement setup for evaluation of a wired 22uF tantalum capacitor. The BNC connectors to the right are the SOL calibration standards.

Figure 3 shows the measurement results in terms of reflection coefficient (S11/Smith chart, blue trace) and series capacitance as calculated from the measured imaginary part of the impedance (S11/C-, red trace). Moreover, the VNWA LCR-meter is shown (bold black figures). The displayed capacitance values are far from the nominal 22uF value. This is because the meter shows the capacitance value averaged over the full frequency range. Therefore, when the LCR meter functionality is being used the frequency span should be restricted close to zero in order to obtain interpretable numbers. Alternatively, one can box-zoom into the frequency range of interest. The LCR meter evaluates the displayed frequency range only.
In the above example the capacitance dramatically drops with increasing frequency to an even negative value, i.e. the capacitor behaves inductive at frequencies above about 400kHz. It is to be expected that the capacitor lead wires start to play an important role in this frequency range.

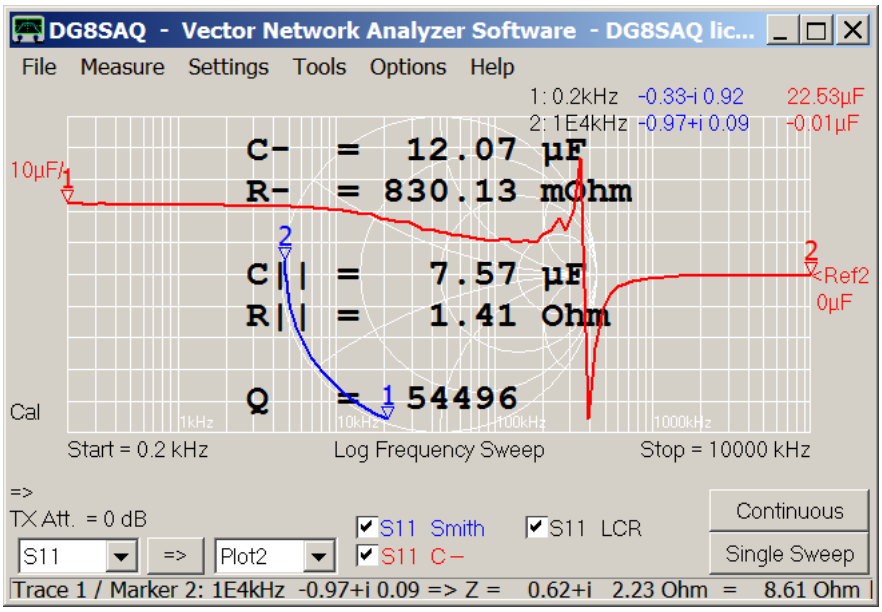

Figure 3: Measurements on the 22uF capacitor shown in Figure 2. Note, that the series equivalent capacitance C- as calculated from the measured impedance (red trace) drops to become even negative. The LCR meter readings (bold black numbers) give numerical values averaged over the full frequency range of 200Hz…10MHz.

トランジスタ技術 2016 年 1 月号～4 月号

USB ネットワーク・アナライザ VNWA3E のすべて<2>～<5>（原文）

The VNWA model fitting tool, which is shown in Figure 4, will help to clarify this. The real capacitor is being modeled as a series circuit of an ideal capacitor, an ideal resistor and an ideal inductor. As can be seen in Figure 5, the model very accurately describes the behavior of the DUT in terms of reflection coefficient (Smith chart). Also, the imaginary part of the impedance is described very accurately, the measurement curve (red) and the model simulation trace (pink) cannot be distinguished. Note, that the real part of the impedance = ESR (effective series resistance, blue trace in Figure 5) is somewhat frequency dependent, which is approximated in the model by a constant R-value. Such a measurement can be used to find a more accurate ESR model.
The fitted parameters also make a lot of sense: C=22,3uF is very close to the nominal capacitance. L=35nH is quite consistent with the parasitic inductance of the lead wires, which is about 1nH per mm by rule of thumb. R=0,82Ω is a reasonable average effective series resistance (ESR) for such a type of component.

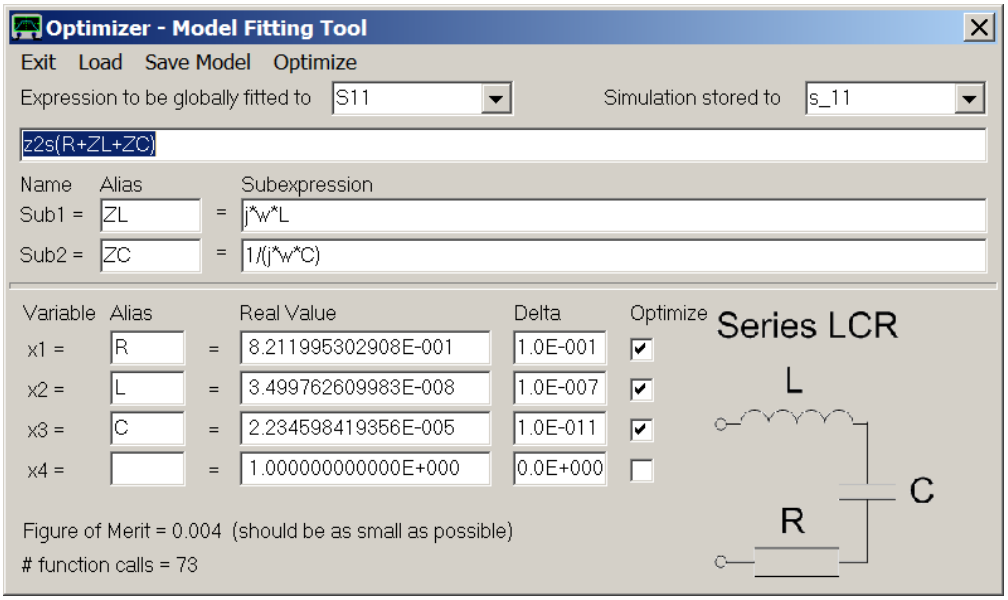

Figure 4: VNWA Model fitting tool used to model the measurements from Figure 3 using a series circuit of ideal capacitor, inductor and resistor.

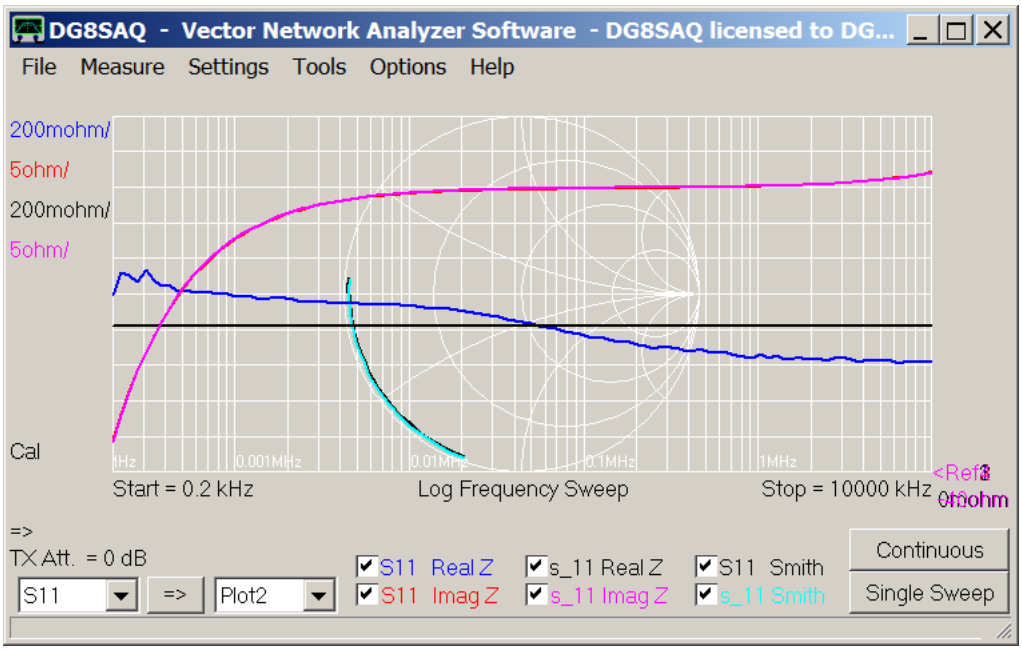

Figure 5: Measurement of the 22uF tantalum capacitor (S11) compared to a simple LCR series circuit model fit (s_11).

2.2 Measuring extremely low impedances

2.2.1 Skin effect in a copper wire

Now, it is attempted to measure the frequency dependent impedance of 11cm of copper wire with 0,3mm diameter. As a dc resistance of only 0,03Ω is expected, an impedance measurement setup is needed that can reliably measure such very low ac impedances. Impedance measurements are normally performed with a VNWA using an impedance bridge (usually built-in) in reflect mode as demonstrated in the previous example. Very low impedances are more accurately measured in shunt mode using a Tee configuration and a transmission measurement, though. Figure 6 shows the basic setup.

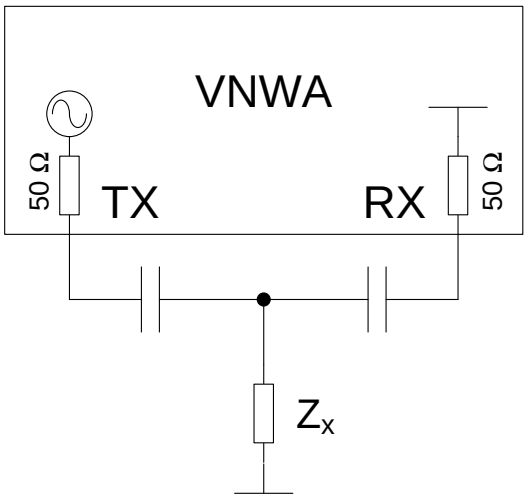

Figure 6: Measuring a very low unknown impedance Z_x in shunt mode using a Tee. Two optional capacitors can be added to serve as dc blocks, if ac impedances are to be measured under the presence of a dc voltage.

The TX and RX lines together with their DC blocking capacitors form a Kelvin probe. Care has to be taken to connect the unknown low impedance with the shortest possible leads to the connection point of the two capacitors, where also the calibration is to be performed. For a shunt mode measurement, in principle only a thru calibration is required, provided the source and load impedances do not deviate from the nominal 50 Ohms over the frequency range of interest. For very low and very high frequency measurements this cannot be taken for granted. Therefore, the VNWA software allows to operate the RX port as a bridge sense input. This operation mode is called “external Bridge” mode and is one of several VNWA3 operation modes shown in Figure 7.

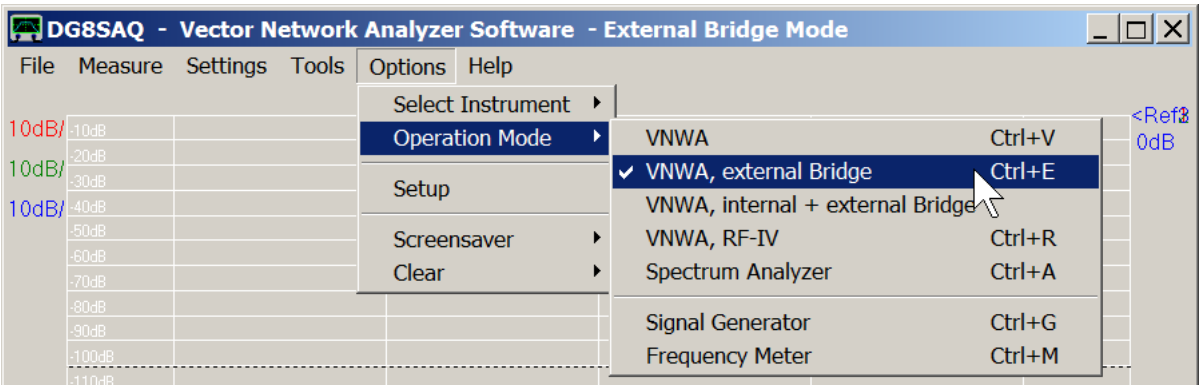

Figure 7: VNWA3 operation modes. For shunt measurements the “external Bridge” mode is selected. The VNWA hardware and software also allows to connect an RF-IV head, which measures current I and voltage V instead of reflection coefficients [2].

The advantage of using “external bridge” mode lies in the fact that a normal SOL calibration can be performed, which corrects for all linear systematic impedance measurement errors introduced by the VNWA hardware itself.

Figure 8 shows a shunt Tee-circuit with the copper wire DUT connected. The wire has been folded in meanders to keep the inductance and thus the imaginary part of the impedance low.

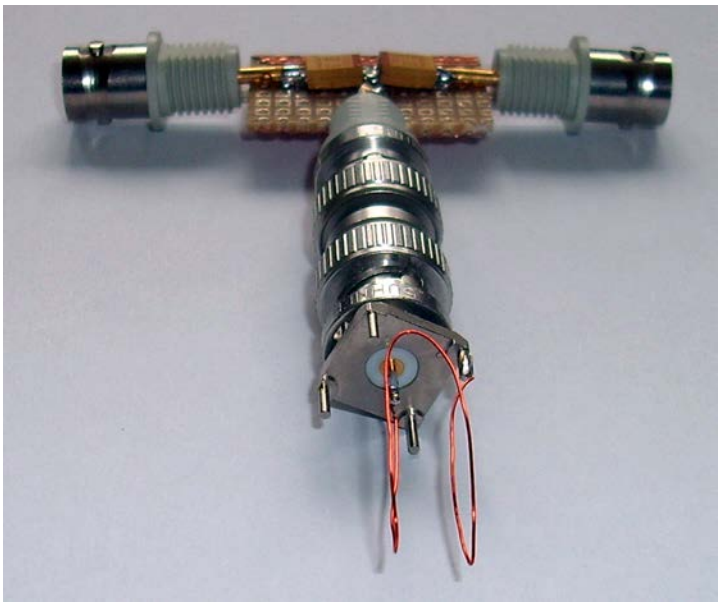

Figure 8: DUT = 11cm copper wire connected to the Tee used to measure the skin effect. The other two Tee-ports are to be connected to the VNWA TX and RX port respectively.

Figure 9 shows the measured real part of the wire impedance (two identical blue traces) and a model fit as shown in Figure 9 (red trace). The theoretical curve and the measurement match very well. Note that the ReZ trace (=custom trace 1) was used to compute the real part of the impedance as reference curve for the optimizer (see Figure 10).

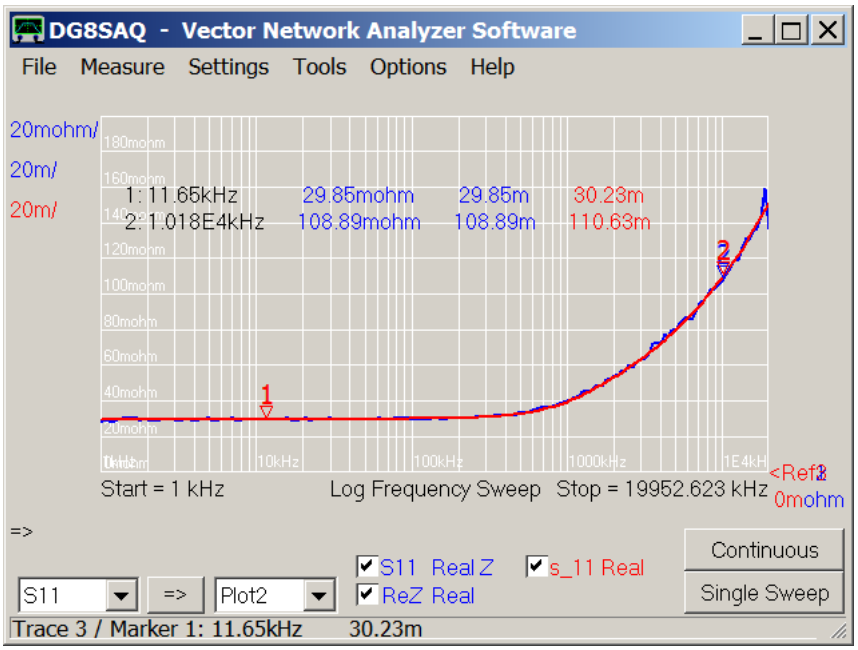

Figure 9: Blue traces: Measured real part of impedance of the copper wire from Figure 8. Red trace: Fitted skin effect model according to [3] as shown in Figure 10.

Figure 10 shows the fitted model, which is the standard skin effect model for a round homogeneous inductor [3]. Only the real part of the impedance has been fitted, as the wire inductivity strongly

depends on the shape of the wire, which is not included. Note, that the model involves complex Bessel function calculus, which can easily be performed with the VNWA software. J0() and J1() denote the Bessel functions of the first kind of order 0 and 1 respectively.

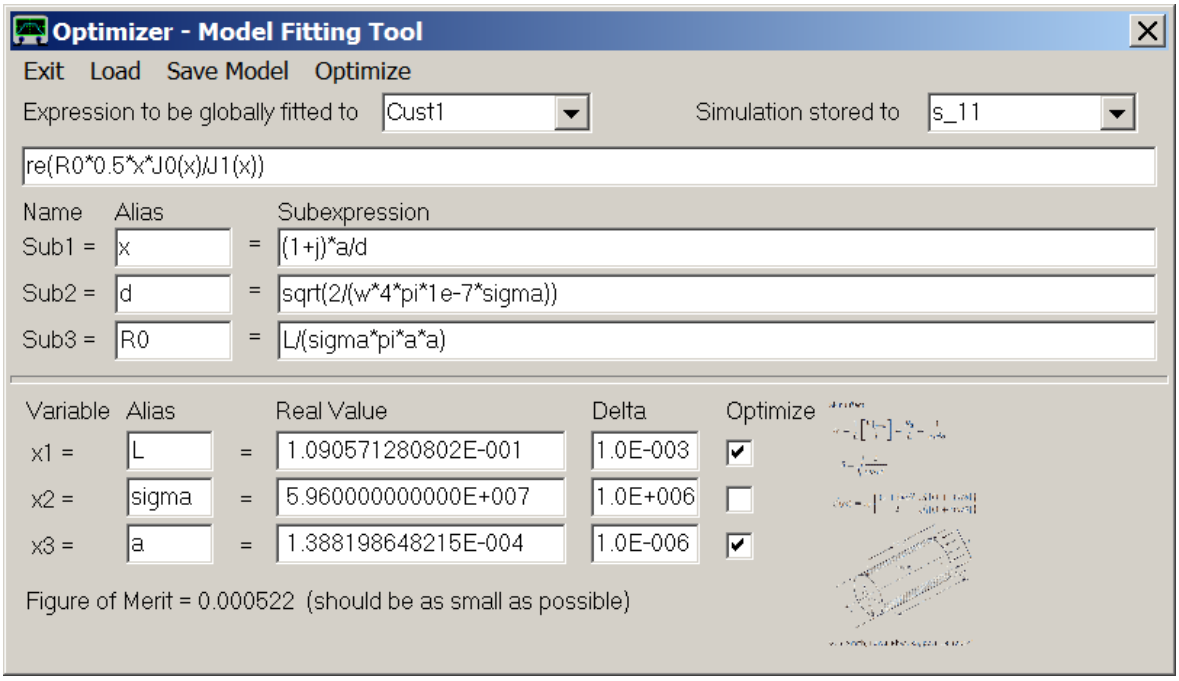

Figure 10: Skin effect fit model according to [3]. L denotes the wire length in m, sigma denotes the wire dc conductivity in S/m and *a* is the wire radius in m. Note, that a descriptive image can be loaded to document the model as seen on the lower right.

The literature value for the dc conductivity of copper was used [4] and not optimized. Only the wire length *L* and the wire radius *a* were varied during the fitting process. The fitted length of 10.9cm matches well with the measured length of 11cm and the fitted radius of 0.14mm matches well with the measured diameter of 0.3mm, which includes the wire isolation coating and thus the wire radius should indeed be below 0.15mm. The subexpression R0 denotes the wire dc resistance formula and d denotes the skin effect penetration depth.

2.2.2 Measuring the stability of power supplies

In this example the impedances of voltage sources and the stability of a voltage regulator are being determined. An ideal voltage source exhibits a source impedance of zero Ohms. When a voltage regulator becomes unstable, the source impedance increases, which can be measured with a VNWA. The frequency range of interest ranges from low audio to HF. The dc blocking Tee shown in Figure 8 is ideally suited to perform such a measurement.

Figure 11 shows a first measurement test on a 9V Li-Ion battery and for comparison on the shorted battery clips. Impedances as low as 10 Milli-Ohms can be measured! The battery has a considerably higher impedance of about 1 Ohm. The increase in impedance at higher frequencies for the battery clip litz wires and the battery itself are likely caused by the skin effect as discussed in the previous section.

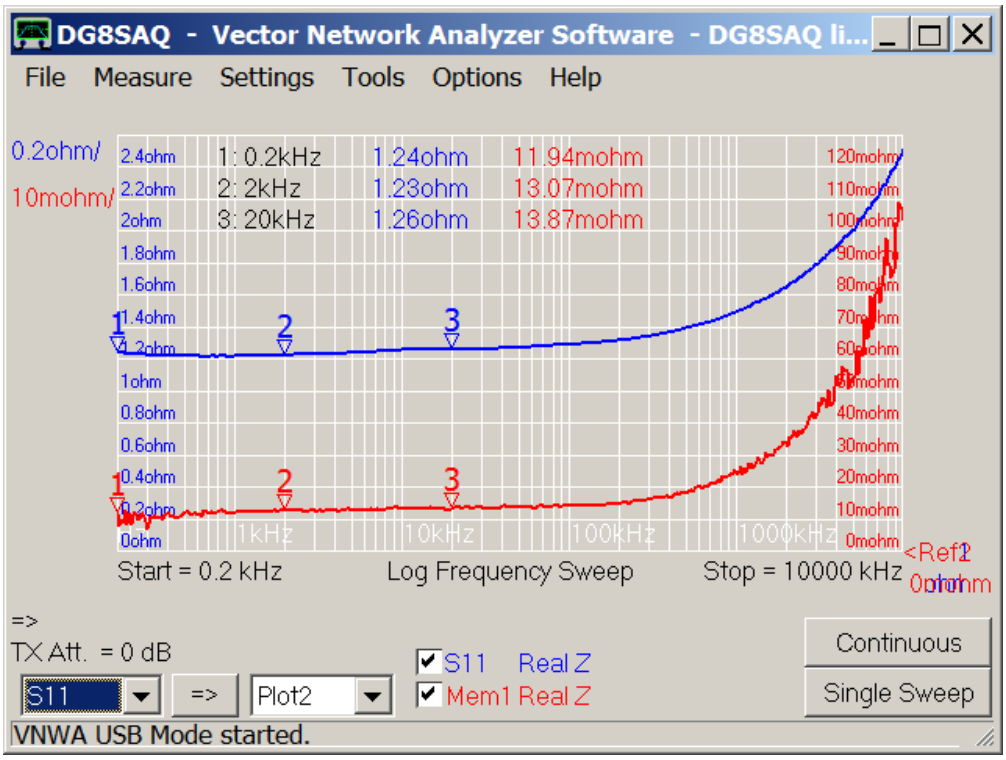

Figure 11: Bode-plot of impedance measurements on a shorted battery clip (red) and on a 9V Li-Ion battery (blue). The traces display the real part of the impedances from 200Hz to 10MHz. Note, that the red trace is scaled in 10 Milli-Ohms per division!

Figure 12 shows two measurements on a TO92 78L05 voltage regulator with 100nF decoupling capacitors on input and output. The blue trace was measured without load current, while the red trace was measured at 50mA output current. For low frequencies, the output impedances are close to zero as expected, but the impedances do peak at higher frequencies indicating a potential instability. Clearly, the regulator becomes more stable as the load current increases.

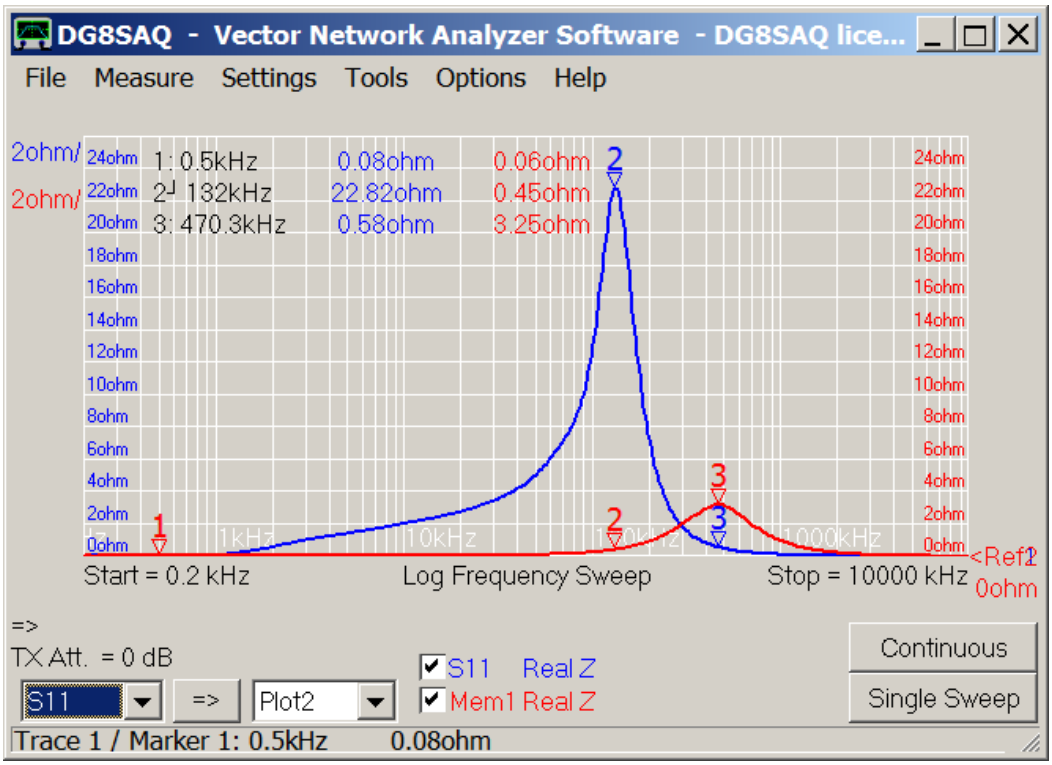

Figure 12: Measured real part of the output impedance of a 78L05 voltage regulator with 100nF decoupling capacitors on input and output. The blue trace was measured without load current, while the red trace was measured at 50mA output current.

As described in [5], the voltage regulator's phase margins can be extracted from these measurements. This can be done in a very convenient way using the VNWA software's powerful numerical capabilities. The procedure is demonstrated with the measurement taken without load current. First, the loaded Q-value of the instability is to be determined from the maximum group delay T_g of the complex impedance data and the frequency f of the group delay peak by:

$$Q = T_g \cdot f \cdot \pi$$

The relevant numbers are being generated by first converting the measured S11 reflection data to impedance data by using a VNWA custom trace, conveniently named Z11 in Figure 13:

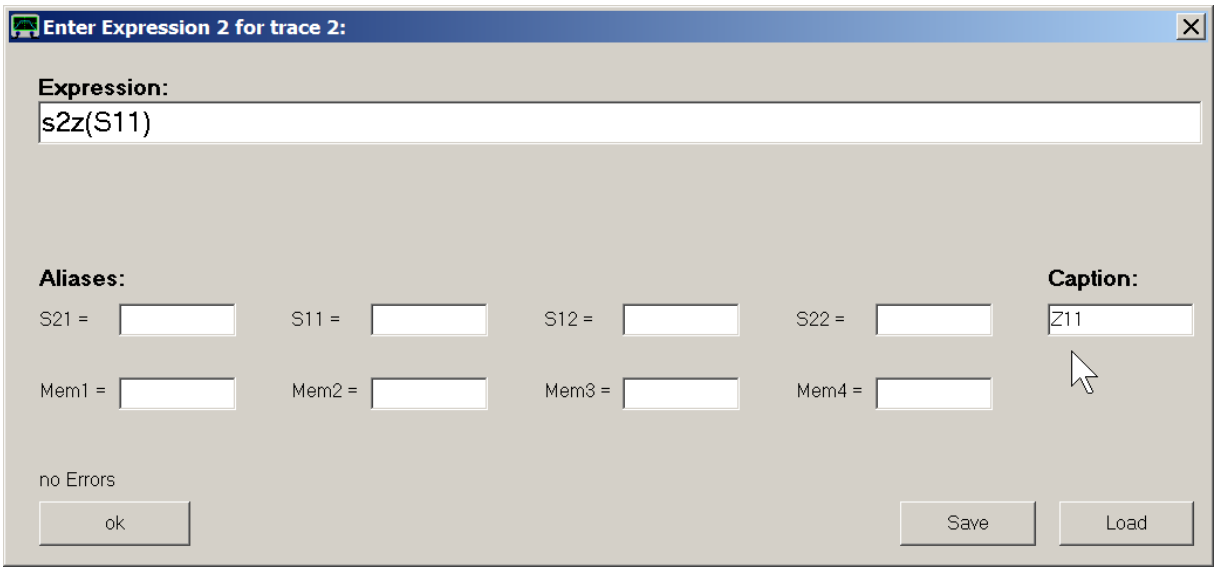

Figure 13: Defining a VNWA custom trace with name Z11, which converts measured reflection data S11 to complex impedance data by means of a conveniently predefined function s2z(). Note, that all VNWA data spaces may be manipulated using complex calculus. The result may be displayed graphically as a custom trace, see e.g. Figure 14.

After this data conversion, the group delay of the calculated impedance Z11 can be displayed as shown in Figure 14. For better visibility, the view has been zoomed into the peak frequency range. A maximum marker has been placed to find the frequency and the delay value of the group delay peak. Note, that a maximum marker always searches the peak of the first trace, which is the blue Z11 trace in Figure 14. The red impedance peak is slightly displaced with respect to the group delay peak.

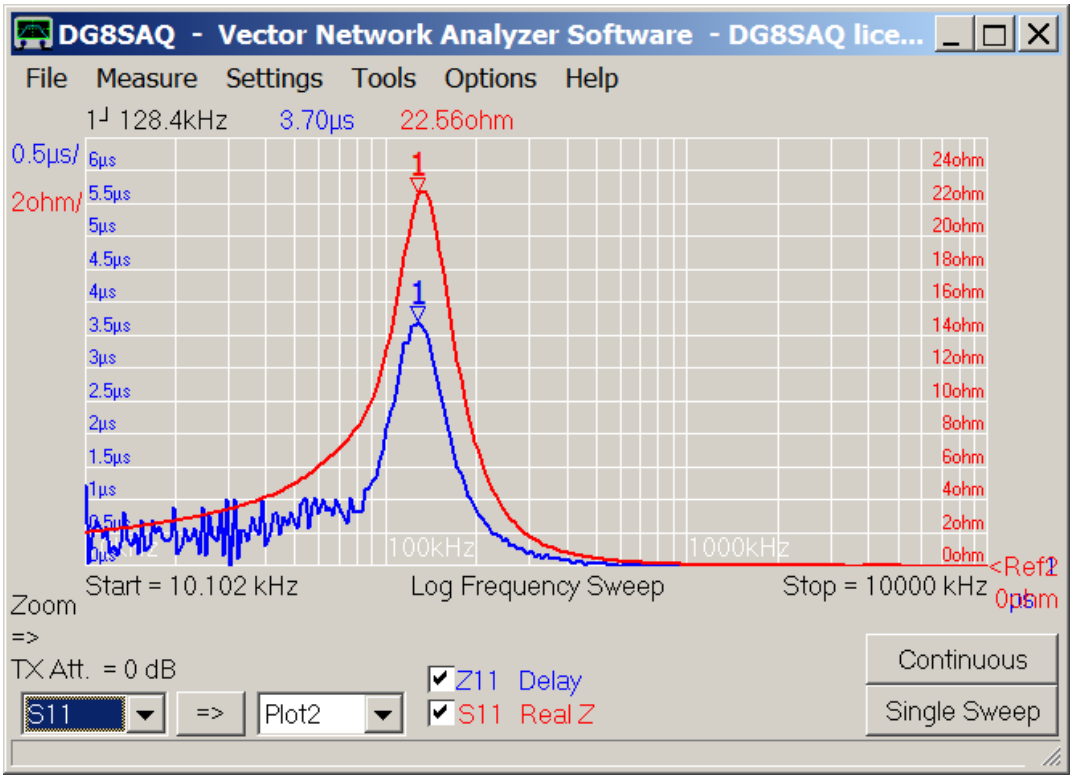

トランジスタ技術 2016 年 1 月号～4 月号

USB ネットワーク・アナライザ VNWA3E のすべて<2>～<5>（原文）

Figure 14: Group delay of the output impedance (blue) and real part of the output impedance (red) of the 78L05 voltage regulator without load current.

The marker values in Figure 14 give all required numbers to calculate Q. Now, the phase margin can be calculated from the Q-value by:

$$\varphi_m(Q) = \arctan\left(\sqrt{\frac{1+\sqrt{1+4Q^2}}{2Q^4}}\right)\cdot\frac{180°}{\pi} \approx 50.36°\cdot Q^{-0.907} \qquad [5]$$

This can conveniently be done using the VNWA's complex calculator tool as shown in Figure 15. The calculator tool allows to directly access measured data and marker data and perform complex valued or real valued calculus. Moreover, it allows to define variables. The "History" panel shows the performed steps. First, the peak frequency is extracted from marker 1 by means of the function *marker(1)* and stored to variable *f*. Second, the peak group delay is extracted from the marker 1 value at trace 1 with the function *mval1(1)* and stored in the variable *tg*. Note, that the function arguments denote the marker number in both cases. In the next step the loaded Q-value is calculated from the previously defined variables and stored in the new variable *Q*. Finally, the phase margin is calculated from Q using the approximate formula from [5]. The phase margin is evaluated to be about 35°. The exact formula has been entered to the "Command" panel but hasn't been evaluated yet. Evaluation of the exact formula yields a similar value of about 33°.

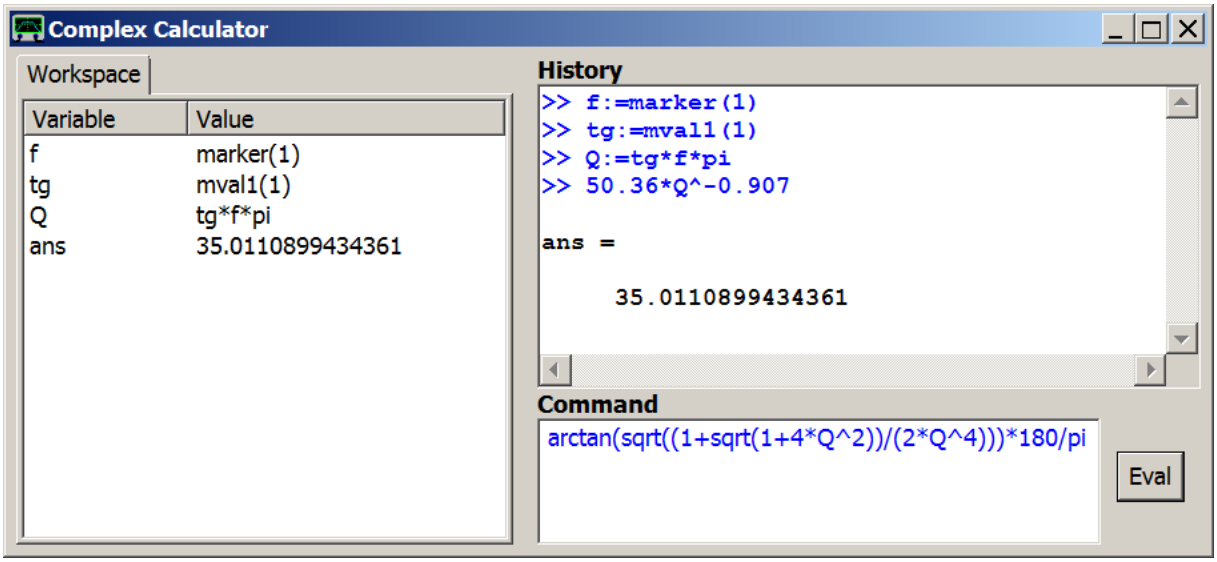

Figure 15: Evaluation of the L78L05's phase margin at zero load current using the complex calculator. The "History" panel shows the performed calculus steps. The exact expression for the phase margin in the "Command" panel has not been evaluated yet. After evaluation, it will yield about 33°.

Of course, this stability measurement has been performed with the rather low impedance of the VNWA ac-loading the power supply via the dc blocking capacitors. Measurements without loading by the VNWA can be performed if a voltage to current converter is being used between TX port and the device under test (DUT) and a high impedance active probe is being used between DUT and RX port. A simpler way to approximate these conditions is to connect high impedance resistors in series with the dc blocking capacitors of the Tee in figure 8. If 1kΩ resistors are being used, the Tee impedance is raised from 25Ω to 500Ω. Of course, the signal amplitude is reduced at the same time by about 26dB

and thus the impedance measurement is expected to become noisier. Figure 16 compares the previous measurements with 25Ω instrument impedance to measurements taken at 500Ω instrument impedance as just discussed.

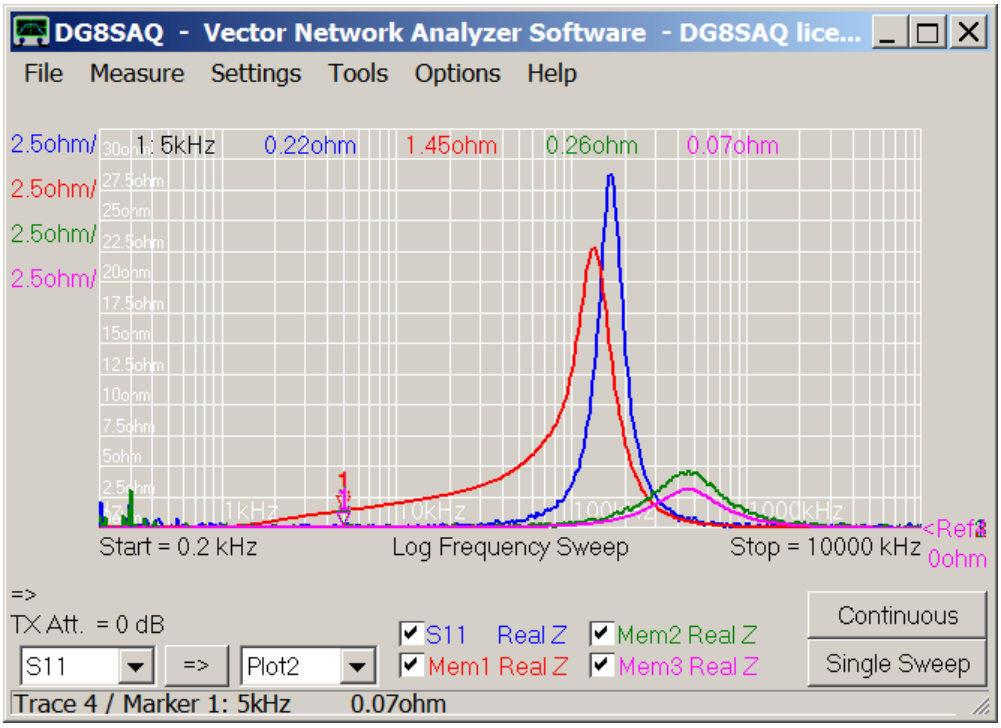

Figure 16: Measured real part of the output impedance of a 78L05 voltage regulator with 100nF decoupling capacitors on input and output at with different load current conditions and VNWA impedances: Blue (S11): 0mA/500Ω; Red (Mem1): 0mA/25Ω; Green (Mem2): 50mA/500Ω; Pink (Mem3): 50mA/25Ω.

Note, that even with the reduced signal amplitude, reliable measurement results can still be achieved. Evidently, the regulator becomes more unstable with increasing instrument impedance. This is to be expected as decreasing the load current yields the same effect. Summarizing, the VNWA3 is well suited to investigate power supply stability.

References

1. Y. Nishimura, “???”, Transistor Technology 4/2015, pp. 69-79.
2. RF-IV test heads are available from e.g. http://www.makarov.ca/ .
3. G. S. Smith, “A simple derivation for the skin effect in a round wire”, Eur. J. Phys. 35, pp.1-13 (2014).
4. http://chemistry.about.com/od/moleculescompounds/a/Table-Of-Electrical-Resistivity-And-Conductivity.htm
5. S. Sandler, “New Technique for Non-Invasive Testing of Regulator Stability” , Power Electronics, available at http://powerelectronics.com/power-electronics-systems/new-technique-non-invasive-testing-regulator-stability

トランジスタ技術 2016 年 1 月号～4 月号

USB ネットワーク・アナライザ VNWA3E のすべて<2>～<5>（原文）